Heliyon 10 (2024) e40784

Contents lists available at ScienceDirect

Heliyon

journal homepage: www.cell.com/heliyon

Research article

Electrocoagulation for nickel, chromium, and iron removal from mine water using aluminum electrodes

Muhammad Ghozali Harahap [a], Muhammad Sonny Abfertiawan [a,*], Mindriany Syafila [a], Marisa Handajani [a], Tonny H. Gultom [b]

[a] Water and Wastewater Engineering Research Group, Faculty of Civil and Environmental Engineering, Bandung Institute of Technology, Indonesia
[b] Program Studi Doktor, Sekolah Ilmu Lingkungan, Universitas Indonesia, Indonesia

ARTICLE INFO

Keywords:
Mine water
Nickel
Chromium
Electrocoagulation

ABSTRACT

High global demand for nickel metal has contributed significantly to the growth of the nickel mining industry in Indonesia. This growth has a positive multiplier effect on the economy, with the potential to affect aquatic life and humans owing to the high levels of chromium, nickel, and iron in mine water. Therefore, this study aims to develop an electrocoagulation (EC) reactor to remove nickel, chromium, and iron from mine water. This study used a continuous reactor and aluminum electrodes with variations in current density (3.378, 6.757, and 10.135 mA/cm^2) and inflow (0.3, 0.5, and 1 L/min). The results showed that the operating scenario with a current strength of 6 A and an inflow of 0.3 L/min had a removal efficiency of 86.89 % nickel, 99.51 % chromium, and 80.61 % iron with a charge loading value of 11,194 F/ma^3 and Reynolds number of 39. These results are expected to provide valuable information for the development of an effective EC technology, thereby demonstrating its potential for the removal of metals from nickel mine water.

1. Introduction

The use of electric vehicles has recently increased owing to global awareness of greenhouse gas emission reductions and the adoption of greener energy. The key component of electric vehicles is the battery, which contributes approximately 35–40 % of the total cost [1]. Therefore, a sustainable supply of nickel as a raw material for battery production is important. As the world's largest Ni producer, Indonesia has abundant reserves, reaching 21 million metric tons (MT) while continuing to experience significant growth. According to data from the United States Geological Survey (2023), Ni production in Indonesia has increased from 345,000 MT in 2017 to 1.6 million MT in 2022. Although this has a positive effect on the economy, it also has the potential to seriously affect the environment.

Water from Ni mining and processing activities is a serious issue that requires urgent attention from all stakeholders. This is due to the presence of dissolved and suspended metals, such as chromium, nickel, iron, and manganese, which can affect water bodies and human health owing to their toxic, mutagenic, and carcinogenic properties [2,3]. Consequently, it is essential to develop an effective and environmentally friendly technology for removing metals from nickel mine water. Several processing methods, such as chemical coagulation, adsorption, ion exchange, reverse osmosis, and membrane filtration, have been applied to overcome this problem

* Corresponding author.
E-mail address: msa@itb.ac.id (M.S. Abfertiawan).

https://doi.org/10.1016/j.heliyon.2024.e40784
Received 14 August 2024; Received in revised form 9 November 2024; Accepted 27 November 2024
Available online 28 November 2024

Abfertiawan et al., 2023; [4,5,6]. However, these methods are beset by high costs, large energy consumption, complexity, or long processes, making the processing of heavy metals difficult Merma et al., 2020.

Owing to these limitations, a reliable and efficient method must be developed to treat mine water while reducing the risk of further contamination. According to Merma et al. [7], electrocoagulation technology is an electrochemical-based water treatment method with a short operating time, minimal chemical consumption, and low sludge production. Various types of wastewaters have been successfully used in this method, including mine water [8,9], domestic wastewater [10,11], electroplating industry wastewater [2,6], and slaughterhouse wastewater [12]. The success of electrocoagulation in treating wastewater contaminated with heavy metals has been demonstrated in previous studies. For example, Stylianou et al. [9] stated that this process could remove Fe (99.9 %), Zn (99.9 %), Mn (99.9 %), Cu (99.9 %), Ni (98 %), Cd (96 %), and Cr (88 %) from mine water using a batch reactor and Al electrodes. Based on El-Ashtoukhy et al. [13], a batch electrocoagulation reactor with Al electrodes removed Ni^{2+} and Cu^{2+} ions from synthetic wastewater with an efficiency of 34.56–100 % under optimum conditions. In the electrocoagulation process, current density and detention time are critical factors in determining the efficiency of wastewater treatment. According to Vargas et al. [14] and Shahedi et al. [15], the removal rate of electrocoagulation reactors increases proportionally with current strength and detention time. These findings indicate that the removal efficiency of heavy metals in wastewater will be enhanced at higher current strength and detention time, attributable to the substantial quantity of metal hydroxide flocs generated in the reactor [16]. Therefore, this study aimed to determine the optimal combination of flow and inflow detention times for removing nickel, chromium, and iron from nickel mine industrial wastewater. The results are expected to facilitate the development of more optimal and sustainable nickel mine water treatment technologies in the future.

2. Materials and methods

2.1. Materials

Mine water samples were obtain right downstream mine activities before sediment ponds from one of nickel mines in Eastern Indonesia. This area has the largest nickel reserves in Indonesia. The samples were collected using the grab sample method and stored in sterile jerry cans at a temperature of 4 °C, as shown in Fig. 1a–c. Subsequently, the samples were sent to the Water Quality Laboratory, Bandung Institute of Technology, for initial characteristic analysis before a maximum storage period of 28 d. The characterization results showed that nickel mine water had a relatively alkaline pH of 7.77 with chromium, nickel, and iron contents of 13.35, 14.45, and 455.5 mg/L, respectively, as presented in Table 1.

2.2. Experimental design and procedure

Experiments were carried out at the Water Quality Laboratory, Environmental Engineering Study Program, Bandung Institute of Technology, using a continuous system electrocoagulation (EC) reactor with a buffer channel flow adapted from Hudori [17]. This reactor consisted of a feed tank, peristaltic feed pump, laboratory-scale EC reactor with a continuous-flow buffer channel system, DC power supply source (model DF 1730 SB, 0–60 V, and 0–20 A), ammeter, voltmeter, and sampling point (Fig. 2a). Additionally, this reactor, composed of transparent acrylic material with a thickness of 5 mm, had a capacity of 21.5 L with dimensions of 20 cm high, 41.4 cm long, and 26 cm wide (Fig. 2b). It also contained 12 aluminum plates (purity of 99.5 %) measuring 23 cm × 20 cm x 0.2 cm (Fig. 2c), arranged monopolar with a distance between electrodes of 3 cm. The plates were immersed to a depth of 14.8 cm with a total effective area of 592 cm^2. The design of the electrocoagulation reactor in this study was engineered to ensure uniform flow distribution and optimal contact between the electrodes and wastewater, thereby facilitating the reaction to occur throughout the reactor volume in a consistent pattern. The electrodes were connected to a direct current (DC) source of 0–20 A and a voltage of 0–60 V. The current and voltage supplies in the EC reactor were monitored using a MASDA DT830B multimeter.

A total of 15 L of artificial mine wastewater samples from the feed tank flowed continuously into the EC reactor through 8 mm polypropylene tubing using a peristaltic pump. The flow rate was set to 0.3–1 L/min to obtain electrolysis times of 15, 30, and 45 min.

Fig. 1. Mine Water runoff: (a) jerrycan sample, (b) mine water, and (c) site location.

Table 1
Characteristics of the nickel mine wastewater.

No.	Parameter	Unit	Original Waste	Artificial Waste
1.	Ni Total	mg/L	14.45	15.48
2.	Cr Total	mg/L	13.35	13.59
3.	Fe Total	mg/L	455.5	283.97
4.	Al Total	mg/L	0.59	0.44
5.	Conductivity	mS/cm	163	921.77
6.	TDS	mg/L	79	477.78
7.	Temperature	°C	25	24.5
8.	pH	–	7.77	5.12

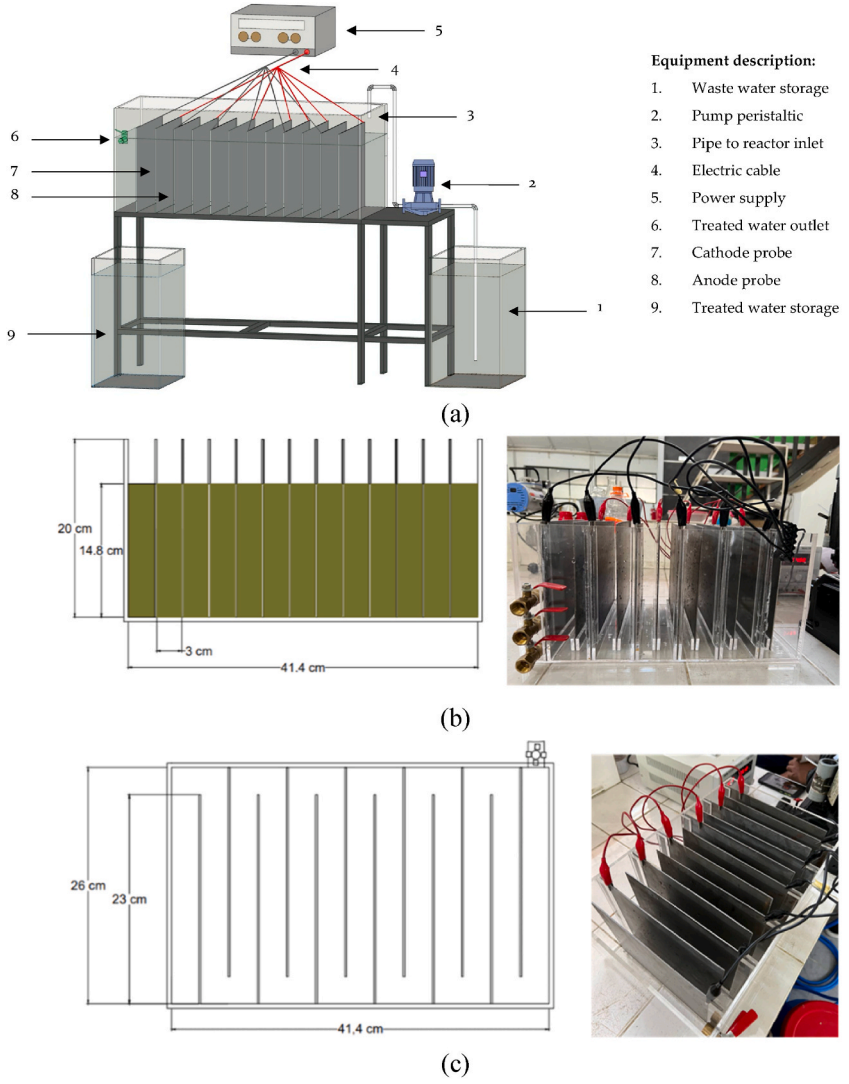

Fig. 2. a) Layout of the continuous system electrocoagulation reactor, b) Electrocoagulation reactor side view, c) Electrocoagulation reactor top view.

Each experiment lasted 120 min, and the total volume of artificial mine wastewater prepared was 60–160 L. The experiments were conducted for 120 min to ensure that the continuous system attained steady-state conditions, thereby ensuring that the results obtained reflected a stable and representative treatment efficiency. The duration of 120 min was selected to allow sufficient time for the treatment process while considering the constraints of laboratory-scale experimentation. Samples of treated mine water were collected every 15 min from the EC reactor effluent tap into a 500 mL beaker and the sediment was allowed to settle for 60 min. The supernatant

samples were collected in 100 mL sample bottles and preserved by adding HNO_3. Subsequently, the pH; conductivity; total dissolved solids; temperature; and total Ni, Cr, Fe, and Al contents were measured. Metal analysis was carried out only on the 120-min sample, considering the steady-state conditions in the continuous system. For each experimental cycle, the electrode was cleaned by soaking it in a 1 M H_2SO_4 solution for 60 min to remove the adsorbed molecules on the electrode surface, followed by rinsing with water.

This study used a 32 factorial (3 × 3) experimental design, including current strength and electrolysis time variations, resulting in a total of 9 experiments with two replications. The variations included current density of 3.378, 6.757, and 10.135 mA/cm^2, and inflows of 0.3, 0.5, and 1 L/min to obtain electrolysis times of 15, 30, and 45 min, respectively. These values were selected based on previous research that removed chromium and nickel using EC technology at a current strength of 0–6 A and detention time of 0–60 min [18].

2.3. Metal analysis methods

Analysis of the total nickel, chromium, iron, and aluminum concentrations in the nickel mine water samples was conducted using Atomic Absorption Spectroscopy (PerkinElmer Analyst 700) according to the EPA 7010 standard method (Graphite Furnace Atomic Absorption Spectrophotometry, Rev. February 0, 2007). Temperature, pH, conductivity, and TDS measurements were carried out using a Portable Multi water quality meter (pH = 0–14, EC = 0–1 mS = m–10 S/m, and 0–100 °C). Sludge samples produced in the EC were collected and separated using a vacuum filter with Whatman 42 filter paper. The solid was dried and stored in a desiccator until further use. The morphology and chemical composition of the dried samples were analyzed using Fourier transform infrared spectroscopy (FTIR), scanning electron microscopy (SEM), and Energy-Dispersive X-ray Spectroscopy (SEM-EDS) at the Water Quality Laboratory, Bandung Institute of Technology.

3. Results and Discussion

3.1. Effect of charge loading

Charge loading (q) is an important parameter in the EC design because it affects the reaction rate and coagulant dose during the process. A high charge loading may result in increased aluminum hydroxide floc formation and Al residues, potentially leading to difficulties in separation and elevated operational costs due to higher energy consumption. Consequently, it is essential to adjust the charge loading based on the characteristics of the raw water and the electrochemical reaction (adapted from Ref. [19]). Charge loading refers to the quantity of charge transferred during electrochemical reactions for a specific volume of water treated and is calculated using Eq (1) [20].

$$CL\left(\frac{F}{m^3}\right) = \frac{I\,x\,t_d}{F\,x\,v} \tag{1}$$

where q is charge loading (CL), I is applied current (A), td is detention time and v is volume of water in the EC reactor (L), F is Faraday's constant (1 F = 96487 C).

The removal efficiency of nickel, chromium, and iron metals as a function of charge loading was presented in Fig. 3. The highest charge-loading value of 11,193 F/m^3 was obtained from variations in the current density of 10.135 mA/cm^2 with an inflow of 0.3 L/min. This shows that a higher charge loading correlates with a greater metal removal efficiency. Based on these results, the best removal efficiency was achieved at the highest charge loading with a final chromium, nickel, and iron concentrations of 0.07 mg/L (99.51 %), 1.99 mg/L (86.89 %), and 51.46 mg/L (80.61 %), respectively.

An increase in the charge loading value can cause a higher increase in the amount of in situ adsorbing coagulant in the form of aluminum oxide ($Al(OH)_3$), following Faraday's law. Subsequently, co-precipitation of metal ions (Ni^{2+}, Fe^{3+}, and Cr^{3+}) forms complex compounds and hydroxide precipitates [21]. This reaction increases metal removal during adsorption because the metal ions replace the OH groups in the $Al_n(OH)3_n$. This produces aluminum, nickel, iron, and chromium hydroxide, as well as complex compounds of aluminum hydroxide and metal ions. These compounds facilitate the removal of metal ions from wastewater through coagulation and precipitation. Similarly, a previous study reported increased arsenic removal efficiency when the charge loading value was more

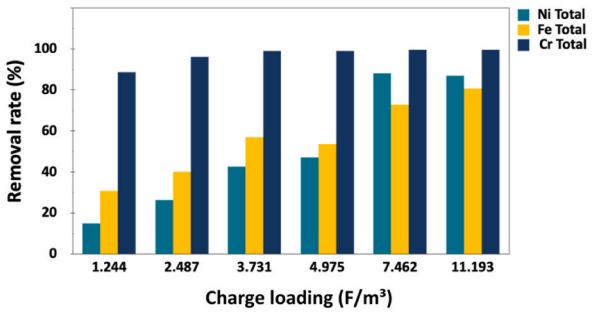

Fig. 3. Effect of Charge Loading on the total nickel, chromium, and iron removal.

significant [19].

3.2. Effect of inflow and current strength

The effect of the flow rate into the reactor at 0.3, 0.5, and 1 L/min or detention times of 45, 30, and 15 min was analyzed for the nickel, chromium, and iron metal removal efficiencies. The current density were 3.378, 6.757, and 10.135 mA/cm^2. The Reynolds number was calculated based on the hydraulic diameter (dh) of the electrochemical cell, derived from its dimensions (41.4 L × 26 W × 20 H, dh = 0.273 m). The density and viscosity of water were assumed to be 997 kg/m^3 and 8.91 × 10^{-4} kg/m.s at 25 °C, respectively. The average flow velocity of the water undergoing treatment (v) and the Reynolds number (Re) were determined using equations (2) and (3).

$$v = \frac{Q}{A} \tag{2}$$

$$Re = \frac{v\, d_h \rho}{\mu} \tag{3}$$

where Q is the volumetric flowrate of the water, and A is the cross-sectional area of each electrochemical cell (41.4 cm × 20 cm), ρ and μ are the density and kinematic viscosity of the water, respectively. Fig. 4 shows the effects of the inflow and current strengths. This figure also shows that the Reynolds number and detention time significantly affected the removal of nickel, chromium, and iron from

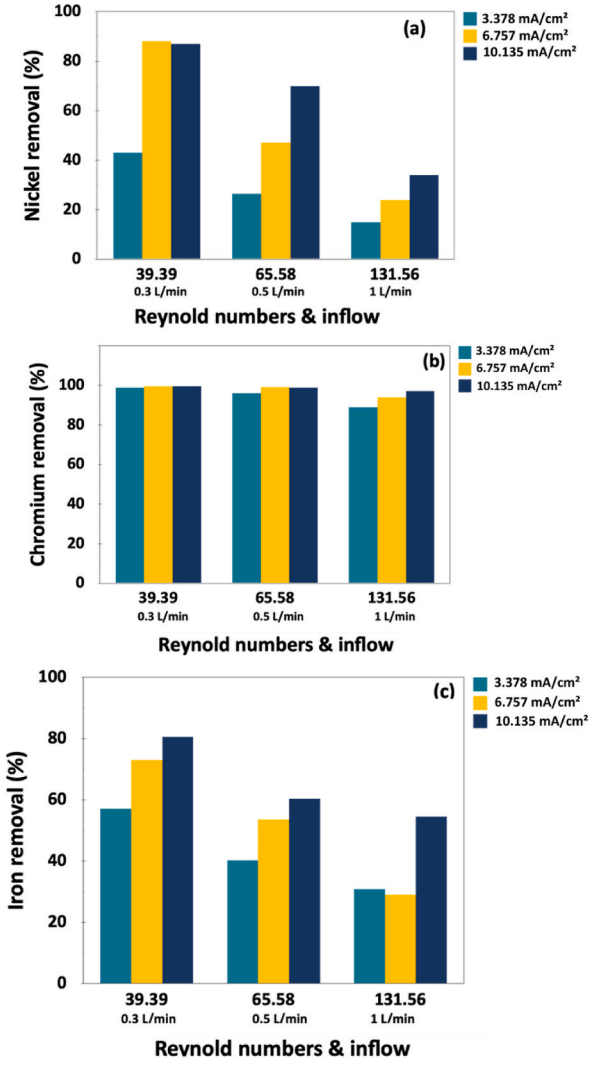

Fig. 4. Effect of inflow, Reynolds number, and current strength on the removal of (a) total nickel metal, (b) total chromium metal, and (c) total iron metal.

mine water. The 10.135 mA/cm^2 current density operating scenario achieved a Reynolds number (Re) of 30, producing the highest metal removal efficiency, i.e., 86.89 % nickel, 99.51 % chromium, and 80.61 % iron. At Re = 30, the resulting flow rate was quite low, causing the metal particles to move in a flow pattern that was regular, sequential, and not excessively turbulent. This caused the metal particles to interact more easily with the flocs produced by the EC process followed by settlement. This process also led to a higher metal removal efficiency because more particles were successfully deposited and separated from the solution. These results are consistent with previous research, where low flow rates with Re values between 39 and 231 (laminar flow) produced a high silica removal efficiency of approximately 80 % at flow rates between 20 and 120 mL/min and a time retention of 112–1125 s [22].

Fig. 4 shows that the removal of Ni, Cr, and Fe decreased at high flow rates with an Re of 130 in all scenarios. This was attributed to floc breakdown owing to the fast flow rate, resulting in a decrease in the removal efficiency. In other cases, when using EC for wastewater treatment at higher rotation speeds, aluminum hydroxide flocs can potentially cause damage and reduce contaminant removal efficiency in wastewater treatment [23].

Competition between metals adsorbed by the coagulant produced in the EC process was observed during the experiment. This was confirmed by the removal efficiencies of the three metals. Fig. 4b shows that the chromium removal efficiency tended to be stable, with a high value of 88–99 % under all conditions. This phenomenon is attributed to the smaller electrode potential value of chromium metal, i.e., −0.28 V, compared to nickel at +1.340 V and iron at −0.440 V [24]. This makes chromium metal more easily reduced and adsorbed by coagulants than other metals. Compared to iron in Fig. 4c, the removal efficiency tended to be lower under all conditions when compared to nickel and chromium. The lower value resulted from a smaller iron reduction potential; thus, its reduction power was relatively weak. Additionally, iron had a higher concentration (265.44 mg/L) than nickel (15.18 mg/L) and iron (13.8 mg/L).

3.3. Sludge formation

Sludge formation in this study was observed visually and not measured analytically. Observations showed that the formation of sludge formation was closely related to inflow and current strength during the experiment in all scenarios. Fig. 5a–i shows that a higher current strength and smaller inflow correlated with more sludge formation. In Fig. 5a and b, with a low current strength of 3.378 mA/cm^2, an inflow of 0.5, and 1 L/min, the flocs settled without floating. This was caused by the low density of hydrogen bubbles produced at low current strengths, which led to upward floc momentum and less effective mixing in the active volume of the EC reactor. Moreover, deposition became dominant, and sedimentation was more efficient than flotation at smaller inflows with higher current strengths, as shown in Fig. 5c–i. With an increase in the current strength from 3.378 to 6.757 mA/cm^2 and 10.135 mA/cm^2, the number of floating flocs increased significantly, as shown in Fig. 5g–i. This increase was caused by the high bubble density at higher current strengths, which improved the pollutant fraction removed by flotation. Reducing the flow rate increased the detention time, providing a longer opportunity for the particles to interact and form flocs, along with high coagulation and settling efficiencies [19,25].

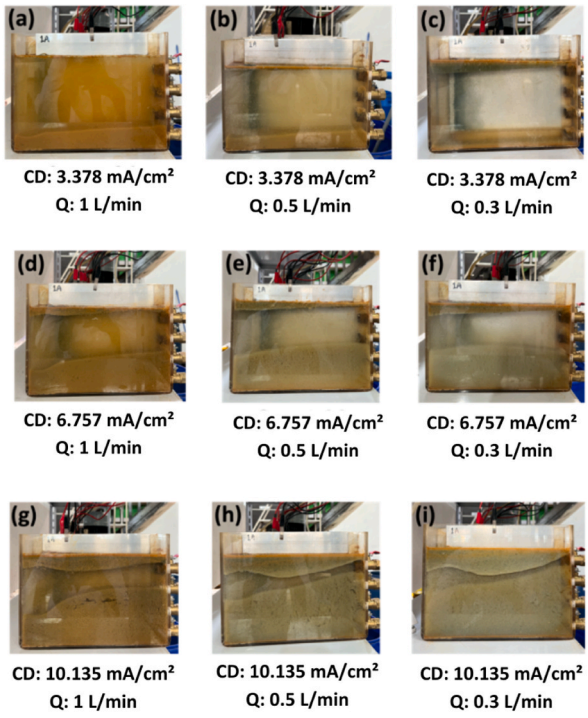

Fig. 5. Effect of current strength (3.378 mA/cm^2 (a–c), 6.757 mA/cm^2 (d–f), and 10.135 mA/cm^2 (g–i)) and inflow (1 L/min, 0.5 L/min, and 0.3 L/min) on sludge formation.

Knowledge of floc behavior and sludge thickness is important for EC performance and designing appropriate post-treatments for sludge removal, such as skimming [26].

3.4. Electrolysis Thermodynamics

During electrolysis, the oxidation reaction was influenced by the cell potential (E°). Half-cell reactions that include electron loss are referred to as oxidation reactions, whereas those that include electron capture are referred to as reduction reactions. At the anode, a greater cell potential correlates with higher oxidation of the compound [27]. The energy used to move electric charges is influenced by the electrode potential, the number of moles of electrons transferred between the electrodes (n), and the electric mutant per mole of electrons, i.e., Faraday's constant (F). The overall energy is calculated by the following Nernst equation Hermawan dan Syafila, 2017:

$$\Delta G = -n * F * E^{o}cell. \quad (4)$$

Based on Eq. (2), when ΔG value < 0, the reaction proceeded spontaneously, whereas at $\Delta G > 0$, the reaction was non-spontaneous. Generally, the type of electrode used in the electrolysis process, including the cell potential that arises during the reaction and the number of electrons, affects the reaction. In this study, aluminum was used as both the anode and cathode. This is because Al is a reactive metal with a cell potential to the left of H_2O, which easily undergoes oxidation reactions. The reduction reaction first occurs at the cathode because of the higher cell potential [28]. In this context, the water reduction reaction occurs after the reduction of Ni^{2+} and Fe^{2+}, whereas at the anode, the oxidation reaction involves Al and H_2O. As the cell potential of Al is lower than that of H_2O, Al oxidation occurs first.

The Gibbs energy (ΔG) analysis results for nickel, chromium, and iron show that the ΔG value for the overall reaction for the three metals was positive ($\Delta G > 0$). This indicates that the Ni, Cr, and Fe removal reactions using the continuous EC system were not spontaneous, implying the need for external energy. Based on these results, the removal of metals using EC requires external energy in the form of an electric current. Specifically, the electric current applied to the electrode produces an in-situ coagulant that reduces and binds metal ions, facilitating the removal of nickel from mine water. As listed in Table 2, the smallest ΔG value for each metal was chromium at 986.26 kJ/mol, followed by nickel at 1907.16 kJ/mol and iron at 2016.85 kJ/mol. This shows that the energy required to remove Cr was smaller than that required to remove Ni and Fe. The removal efficiency was directly proportional to the ΔG value of each metal. Therefore, smaller ΔG values correlate with lower energies required to remove pollutants and higher efficiency.

3.5. Elimination kinetics

In this investigation, the kinetics of nickel, chromium, and iron metal removal were examined utilizing removal data under conditions that yielded the highest removal efficiency, specifically employing a current density variation of 10.135 mA/cm^2 and inflow of 0.3 L/min with an electrolysis time of 45 min. From the experimental results, the removal kinetics reaction for Ni metal was a first-order reaction at a rate of 0.0211/minute ($R^2 = 0.8901$) as listed in Table 3. This indicates that the reaction rate is mainly influenced by the Ni concentration in the mine water. Therefore, a higher Ni concentration correlates with a faster EC reaction. Other factors, such as variations in the current strength and detention time, have less influence on the nickel removal rate [29]. In first-order reaction kinetics, the main mechanism is physisorption [30], in which nickel cations are removed by adsorption on the surface of aluminum hydroxide flocs [31]. Kim et al. [30] also reported that a first-order kinetic reaction occurred during the removal of nickel from metal plating wastewater using iron and aluminum electrodes with a current density of 2–4 mA/cm^2. However, Moersidik et al. [32] reported that the reaction kinetics of nickel removal from electroplating wastewater using aluminum electrodes with a current density of 20 mA/cm^2 is second order. This difference can be attributed to the use of various types of electrodes and current densities in the experiments.

Based on the analysis of Cr and Fe, the kinetic equation from the experimental data indicated a second-order reaction. For chromium, the rate from the second-order reaction was 0.0799/min with an R^2 of 0.4921, whereas that of iron was 0.0001/min at an R^2 of 0.9898. The chromium removal rate was greater than that of iron. This indicates that EC can remove Cr more quickly than Fe. Kim et al. [30] described a second-order kinetic model that refers to the metal removal mechanism in EC through chemisorption. The results showed that the removal of chromium and iron from EC occurs through a chemisorption process. In this mechanism, chromium and iron ions are chemically adsorbed onto the surface of aluminum hydroxide to form a bimetallic hydroxide mixture. During the co-precipitation reaction, metal-OH and metal-O-metal bonds formed, which play a significant role in the removal of Cr and Fe from wastewater.

Table 2
Results of Gibbs (ΔG) energy analysis.

Parameter	ΔG total
Total Ni	1907.16 kJ/mol
Total Cr	986.16 kJ/mol
Total Fe	2016.85 kJ/mol

Total $\Delta G > 0$ (reaction is not spontaneous).

Table 3
Kinetics of total nickel, chromium, and iron removal.

Order	Nickel		Chromium		Iron	
	K (/minute)	R^2	K (/minute)	R^2	K (/minute)	R^2
0	−0.1032	0.8052	−0.0611	0.3018	−1.4555	0.7741
1	**0.0211**	**0.8901**	0.0249	0.3526	0.0128	0.9406
2	0.0065	0.724	**0.0799**	**0.4921**	**0.0001**	**0.9898**

3.6. Sludge characteristics

3.6.1. FTIR analysis

Fig. 6 shows the FTIR results for the sludge precipitated using the EC process at a current density of 10.135 mA/cm^2, an inflow of 0.3 L/min, and a detention time of 45 min. All spectra showed peaks at approximately 2500–4000 cm^{-1}, which indicated the presence of OH stretching in the sludge samples. This indicated the formation of metal hydroxide species in the sludge samples during EC. The peak at approximately 3425.58 cm^{-1} indicated the OH stretching of water associated with the $Al(OH)_3$ species in the sludge. A sharp peak at 1639 cm^{-1} appeared as a result of the bending vibration of H-O-H, whereas the peak at 1118.71 cm^{-1} was attributed to C-O stretching. Additionally, the peak at 977.91 cm^{-1} indicated aromatic C-H bending while the peak at 609.51 cm^{-1} revealed the presence of metal oxides in the EC sludge. The FTIR data showed that most of the Al released during the EC process was included in the adsorption, complexation, and precipitation reactions, which play a role in removing metal from the solution [33].

3.6.2. SEM analysis

Fig. 7a–c shows the floc morphology at magnifications of 1,500x, 3,500x, and 7,000x before processing. Initially, these flocs appeared to be arranged in uniform and unified lumps; however, the particles became irregular after the EC process, as shown in Fig. 7d–f. The pores in the sludge produced after the EC process indicated trapping and adsorption phenomena, along with porous characteristics. Flocs are amorphous, loose, and porous, and have a large porosity and specific surface area, showing a good adsorption ability [34].

3.6.3. EDS analysis

EDS analysis was used to examine the composition of the main elements adsorbed on the aluminum hydroxide in the EC sludge, as shown in Fig. 8. In this spectrum, Al, Fe, Ni, Cr, and oxygen in the floc are shown at 50, 4.51, 0.88, 0.18, and 70.66 %, respectively. Aluminum dominates after oxygen in EC sludge, with a percentage of approximately 19.50 %. The EDS results showed the presence of Ni, Cr, and Fe adsorbed on aluminum hydroxide. Furthermore, other elements detected were chemicals used in testing and contaminants on the anode and cathode, such as sulfur (4.17 %) obtained from artificial waste chemical reagents as $FeSO_4$. Lu et al. [35] reported the presence of 13.29 % aluminum in sludge produced from the adhesive wastewater treatment process. These aluminum metal ions are produced through an anodic dissolution process, forming various metal hydroxy complexes, both mononuclear and multinuclear, in electrolytic cells. Some examples include $Al(OH)_4^-$, $Al(OH)_2^+$, $Al(OH)^{2+}$, $Al_2(OH)_4^{2+}$, $Al_6(OH)_{15}^{3+}$, $Al7(OH)_{17}^{4+}$, $Al_8(OH)_{20}^{4+}$, $Al_{13}(OH)_{34}^{5+}$, and $Al_{13}O_4(OH)_{24}^{7+}$, which transform into $Al(OH)_{3(s)}$ precipitates through a complex precipitation kinetics process [36,37]. All components containing aluminum have a sufficiently large surface area that is conducive to the fast adsorption of iron, nickel, and chromium metals, as well as for capturing colloidal particles in aqueous media. This process leads to the removal of dissolved chemicals and colloidal particles via precipitation [38]. After characterizing EC sludge using FTIR and SEM-EDX analyses, Goren and Kobya [33] and Kumari and Kumar [39] observed that aluminum formed a complex with pollutants, leading to deposits in the processing unit.

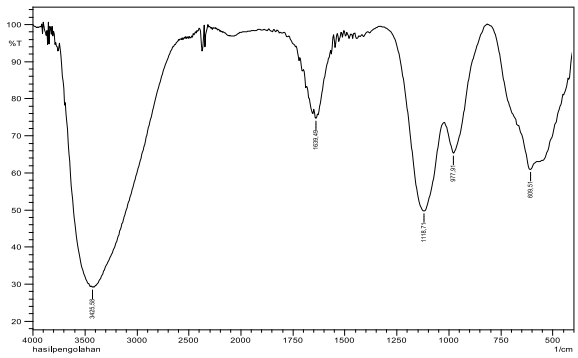

Fig. 6. FTIR analysis of sludge after the EC process.

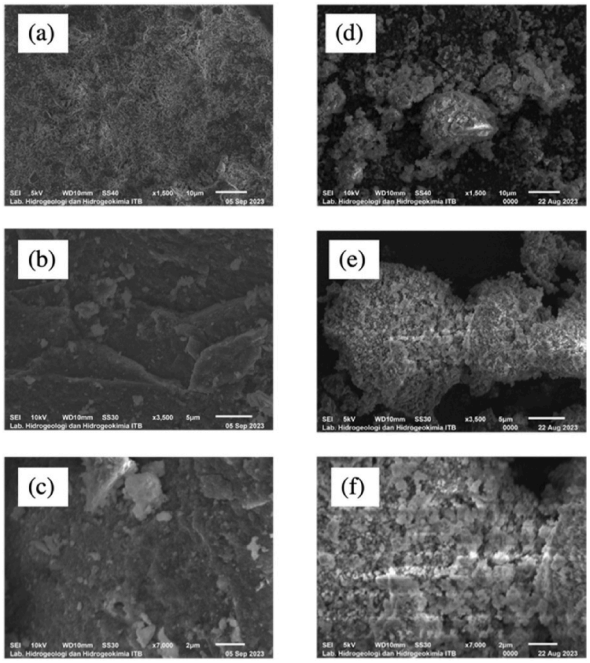

Fig. 7. SEM images of the sludge surface morphology (a–c) before EC and (d–f) after EC.

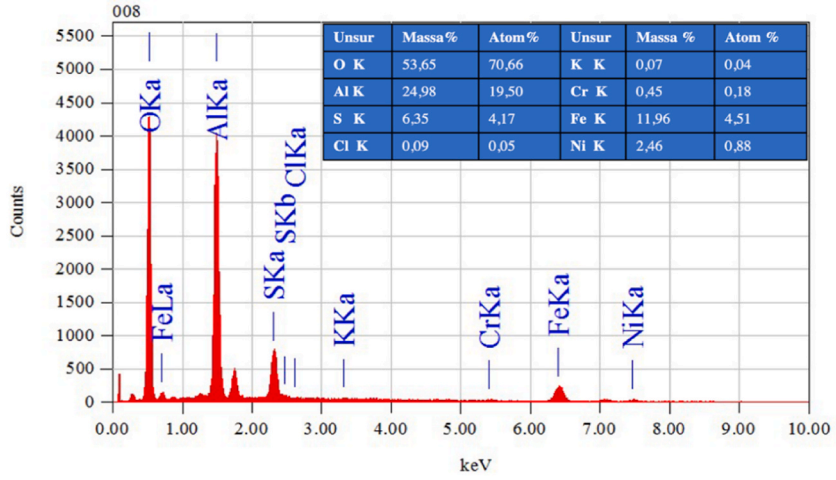

Unsur	Massa%	Atom%	Unsur	Massa %	Atom %
O K	53,65	70,66	K K	0,07	0,04
Al K	24,98	19,50	Cr K	0,45	0,18
S K	6,35	4,17	Fe K	11,96	4,51
Cl K	0,09	0,05	Ni K	2,46	0,88

Fig. 8. EDS analysis of the sludge after the EC process.

3.7. Change in mass of aluminum electrode

In this study, the type of electrode utilized for the continuous EC was an aluminum plate with a purity of ±98.5 %. Fig. 9 illustrates the electrode morphology captured by SEM on the anode surface before and after the electrocoagulation process. As observed in Fig. 9a and (b), the anode electrode surface prior to EC testing exhibited a smooth texture with no visible porosity in the aluminum microstructure. Conversely, Fig. 9c and (d) reveals a rough electrode structure with a surface characterized by numerous small cavities. This phenomenon is attributed to the dissolution of electrode metal into the solution during the electrocoagulation process, resulting in the formation of voids on the surface. Analysis of physical changes in aluminum electrodes was also conducted by comparing the concentration of aluminum in artificial mine wastewater before and after treatment, mass loss of aluminum electrodes, theoretical and experimental energy consumption, and the release rate of Al^{3+}. The concentration of aluminum in artificial mine wastewater before and after treatment can be observed in Fig. 9.

Fig. 9 demonstrates an increase in aluminum (Al) concentration in nickel mine wastewater across all experiments. This observation indicates that during the electrocoagulation process, Al ions are dissolved from the electrode, effectively binding Ni, Cr, and Fe metals

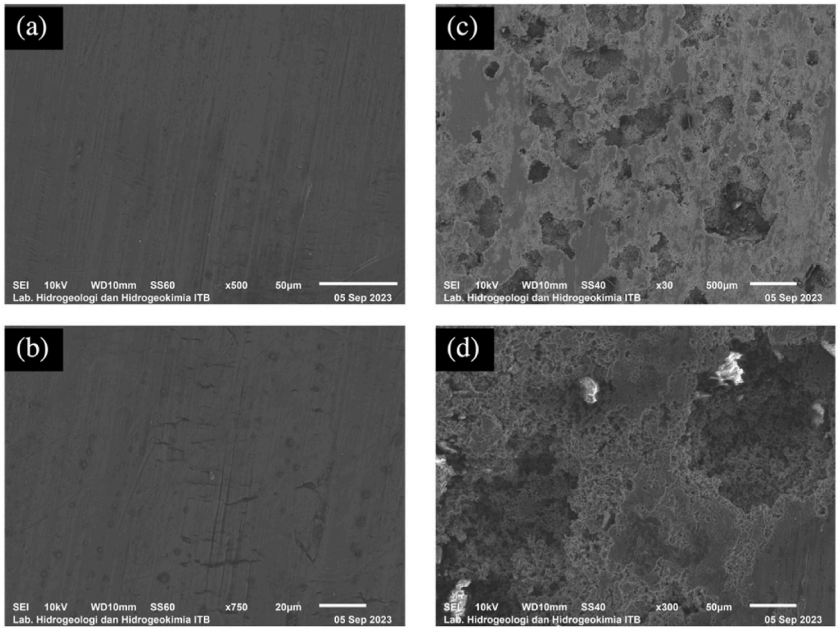

Fig. 9. SEM of anode electrode surface (a–b) before EC, (c–d) after EC.

and forming sludge. Although an increase in Al concentration is observed, this does not reflect a system failure; rather, it suggests that a greater quantity of dissolved Al ions is available for interaction with other contaminants. With the Al concentration remaining within normal limits for wastewater, these results confirm that the electrocoagulation process has successfully enhanced the availability of Al ions, which is crucial in the coagulation mechanism. Consequently, the elevated Al concentration post-treatment can be interpreted as a positive indicator of the electrocoagulation reaction's efficacy in improving wastewater quality. Mass loss of Al electrodes was analyzed by calculating the difference in total weight of 12 electrodes before and after processing in each experiment, and the results are presented in Fig. 10.

Fig. 11 demonstrates that at lower flow rates (0.5 and 0.3 L/min), the mass loss of Al electrodes increases with rising current density, reaching maximum values at a current density of 10.135 mA/cm^2 (14 g and 17 g, respectively). This indicates that lower flow rates with longer detention times facilitate more efficient Al ion release, supporting higher removal of Ni, Cr, and Fe metals, as observed in previous analyses. The increased Al ion release at lower flow rates also signifies that more Al ions are available to react with pollutants such as Ni, Cr, and Fe metals, enhancing the formation of flocs and sludge that bind these pollutants. In other words, low flow rates and high current densities effectively increase the removal of Ni, Cr, and Fe metals through precipitate formation, while Al consumption from the electrodes increases. Therefore, a balance between flow rate and current density must be achieved to optimize the removal of Ni, Cr, and Fe metals while minimizing excessive Al electrode consumption. From the aluminum electrode mass loss data, the concentration of aluminum dissolved in the wastewater was obtained, enabling the calculation of the aluminum electrode release rate for each current density variation, with the results presented in Table 4.

As observed in Table 4, an increase in current strength during the electrocoagulation process enhances the release rate of Al^{3+} ions, attributable to the acceleration of electrochemical reactions at the electrodes. Higher current strengths generate increased electrochemical energy, elevated electrode potentials, and intensified agitation within the system, all of which contribute to the accelerated release of Al^{3+} ions. Furthermore, increased current strength may engage a greater number of active electrodes in the process, thereby augmenting the total capacity for metal ion release. This phenomenon plays a crucial role in improving the efficiency of heavy metal removal from wastewater through electrocoagulation.

3.8. *Two-Way Anova analysis*

This study conducted a significance test on the effect of independent variables, i.e., current strength and inflow, on the nickel, chromium, and iron removal efficiency. To determine the significance effect, Two Way ANOVA was used with a significance level of $\alpha = 0.05$, where a p-value of less than 0.05 showed a significant effect. The results demonstrated that the variable flow rate exerted a significant influence on the variability of metal removal for all metals examined, in conjunction with other factors such as current density, which plays a crucial role in the electrocoagulation process, as delineated in Table 5. Fig. 4 confirms this analysis, where a significant change was observed in the removal of all metals when the inflow increased from 0.3 to 0.5 and 1 L/min.

These results correlate with those of a previous report that investigated the effect of inflow on the detention time for metal removal from wastewater. Liu et al. [40] reported increased nickel removal in EC by increasing the detention time from 10 to 60 min at a current density of 30 mA/cm^2, pH of 4, and using aluminum electrodes. Singh Thakur et al. [41] found an increase in the chromium

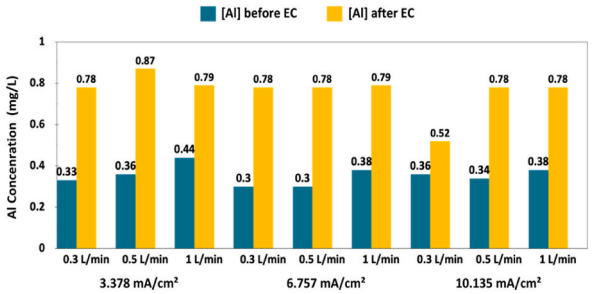

Fig. 10. Effect of inflow and current density on the concentration of aluminium.

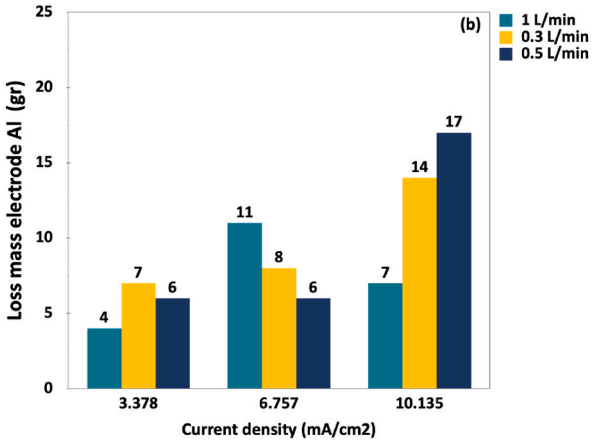

Fig. 11. Effect of current density and inflow on the loss mass of aluminium.

Table 4
Rate of aluminum ion release.

Current density	Al^{3+}Electrode Ion Release Rate (mg/min)	R^2
3.378 mA/cm^2	3,9	0,9404
6.757 mA/cm^2	1933	0,946
10.135 mA/cm^2	12,23	0,9993

Table 5
Two-way ANOVA results for the optimum EC scenario experiment.

Independent Variable	Nickel Removal		Chromium Removal		Iron Removal	
	F value	P-value	F value	P-value	F value	P-value
Strong currents	5.345	0.0691	2.2015	0.3311	125.55	**< 0.001**
Inflow	10.667	**0.0048**	10.257	**0.0059**	61.35	**< 0.001**

Values in bold indicate P-values <0.05 obtained in each experiment.

removal efficiency by increasing the detention time from 20 to 40 min at a current density of 140 A/cm^2, pH of 5, and using iron electrodes. Additionally, Doggaz et al. [42] reported a high iron removal efficiency with an increase in the detention time from 20 to 60 min at a current density of 2.5 mA/cm^2, pH of 5, and using aluminum electrodes. This significant correlation can be attributed to the smaller inflow, which increased the electrolysis time and the amount of metal hydroxide, OH^-, and H_2 bubbles produced by the electrode during the EC process. This resulted in a greater contaminant absorption capacity and increased floc formation, thereby increasing the pollutant removal efficiency [43].

Based on the Two-Way ANOVA analysis results in Table 5, the current strength variable shows a p-value of >0.05 for the removal of nickel and chromium. The p-value for iron was less than 0.05, indicating that the current density only had a significant effect on iron removal. Fig. 4c confirms this effect, where the iron removal efficiency increased from 28 to 73 % at a current density of 6.757 mA/cm^2 to 81 % at 10.135 mA/cm^2 with an inflow of 0.3 L/min. Variations in the current strength were observed to significantly influence iron

removal owing to the increase in $Al(OH)_3$ production by the aluminum electrode. $Al(OH)_3$ functions as a coagulant that adsorbs metal iron particles from wastewater, thereby increasing its efficiency. Similarly, Alam et al. [8] observed a significant increase when the current strength was increased from 6 to 18 V at an electrolysis time of 45 min and pH of 2.83 using aluminum electrodes. A high current strength increases the production of $Al(OH)_3$, which plays an important role in adsorbing metal particles and increasing the removal efficiency. These results demonstrate the importance of controlling the current strength in the EC process to increase the removal efficiency of heavy metals from wastewater.

4. Conclusion

In conclusion, this study investigated the application of electrocoagulation (EC) reactor to remove chromium, nickel, and iron from mine wastewater. The results showed that the operating conditions at a current density of 10.135 mA/cm^2, inflow of 0.3 L/min, and detention time of 45 min produced the highest removal efficiencies of 86.89, 99.51, and 80.61 %, for chromium, nickel, and iron with a charge loading value of 11.194 F/m^3 and Re of 39.39, respectively. The final concentration of chromium met the quality standards, whereas nickel and iron did not fulfill the quality standards (0.5 mg/L for nickel and 5 mg/L for chromium). The nickel removal kinetics that were most consistent with the experimental data were a first-order reaction with a rate of 0.0211/min ($R^2 = 0.8901$). For chromium and iron, the second-order reaction was most suitable. For Cr, the reaction rate was 0.0799/min with an R^2 of 0.4921, whereas iron was 0.0001/minute with an R^2 of 0.9898. These results show that EC technology can be developed to remove the metals contained in nickel mine water. Moreover, future research should be conducted using real Ni mine water to determine phenomena that may not be visible during laboratory experiments. Furthermore, solar-powered EC could be developed into an effective, efficient, and environmentally friendly technology, facilitating its application in the mining industry in tropical countries with high sunshine durations.

CRediT authorship contribution statement

Muhammad Ghozali Harahap: Writing – original draft, Methodology, Investigation, Formal analysis, Data curation. **Muhammad Sonny Abfertiawan:** Writing – review & editing, Writing – original draft, Visualization, Validation, Supervision, Resources, Project administration, Methodology, Investigation, Funding acquisition, Formal analysis, Data curation, Conceptualization. **Mindriany Syafila:** Writing – review & editing, Methodology, Data curation, Conceptualization. **Marisa Handajani:** Writing – review & editing, Data curation, Conceptualization. **Tonny H. Gultom:** Project administration, Funding acquisition, Conceptualization.

Data and code availability Statement

Data included in article/supplementary material is referenced in the article.

Declaration of competing interest

The authors declare that they have no known competing financial interests or personal relationships that could have appeared to influence the work reported in this paper.

Acknowledgments

This study was supported by the Bandung Institute of Technology through the Water and Wastewater Engineering Research Group (KK-RALC), Faculty of Civil and Environmental Engineering research grant as part of the program titled "Program Penelitian dan Pengabdian kepada Masyarakat (P2MI) ITB 2023."

References

[1] G. Zhao, X. Wang, M. Negnevitsky, Connecting battery technologies for electric vehicles from battery materials to management, iScience 25 (2) (2022) 103744, https://doi.org/10.1016/j.isci.2022.103744. Elsevier BV.
[2] J.M. Costa, J.G.R. dos da Costa, A.F. dan de Almeida Neto, Techniques of nickel (II) removal from electroplating industry wastewater: overview and trends, Journal of Water Process Engineering 46 (2022) 102593, https://doi.org/10.1016/j.jwpe.2022.102593.
[3] Ibtisani Farahnaz, Muhammad Sonny Abfertiawan, Mindriany Syafila, Marisa Handajani, Firman Gunawan, Febriwiadi Djali, Metals distribution in river sediment from open-pit coal mine activity, in: P. Stanley, C. Wolkersdorfer, K. Wolkersdorfer, E. Mugova (Eds.), IMWA 2023 – Y Dyfodol | the Future, International Mine Water Association), Newport, Wales, UK, 2023, pp. 159–165.
[4] Muhammad Sonny Abfertiawan, Faiz Hasan, Marisa Handajani, Mindriany Syafila, Firman Gunawan, Febriwiadi Djali, High total suspended solid (TSS) removal for coal mining water using electrocoagulation, in: P. Stanley, C. Wolkersdorfer, K. Wolkersdorfer, E. Mugova (Eds.), IMWA 2023 – Y Dyfodol | the Future, International Mine Water Association), Newport, Wales, UK, 2023, pp. 1–5.
[5] M.S. Abfertiawan, M. Syafila, M. Handajani, F. Hasan, H. Oktaviani, F. Gunawan, dan F. Djali, Batch electrocoagulation process for the removal of high colloidal clay from open-cast coal mine water using Al and Fe electrodes, Mine Water Environ. 43 (3) (2024) 516–528, https://doi.org/10.1007/s10230-024-01004-1. Springer Science and Business Media LLC.
[6] L. Xu, X. Xu, G. Cao, S. Liu, Z. Duan, S. Song, M. Song, M. Zhang, Optimization and assessment of Fe–electrocoagulation for the removal of potentially toxic metals from real smelting wastewater, J. Environ. Manag. 218 (2018) 129–138, https://doi.org/10.1016/j.jenvman.2018.04.049. Elsevier BV.
[7] A.G. Merma, B.F. Santos, A.S.C. Rego, R.R. Hacha, M.L. Torem, Treatment of oily wastewater from mining industry using electrocoagulation: fundamentals and process optimization, J. Mater. Res. Technol. 9 (6) (2020) 15164–15176, https://doi.org/10.1016/j.jmrt.2020.10.107. Elsevier BV.

[8] P.N. Alam, Yulianis, H.L. Pasya, R. Aditya, I.N. Aslam, K. Pontas, Acid mine wastewater treatment using electrocoagulation method, Mater. Today: Proc. 63 (2022) S434–S437, https://doi.org/10.1016/j.matpr.2022.04.089. Elsevier Ltd.

[9] M. Stylianou, E. Montel, A. Zissimos, I. Christoforou, K. Dermentzis, A. dan Agapiou, Removal of toxic metals and anions from acid mine drainage (AMD) by electrocoagulation: the case of North Mathiatis open cast mine, Sustainable Chemistry and Pharmacy 29 (2022) 100737, https://doi.org/10.1016/j.scp.2022.100737.

[10] P. Patel, S. Gupta, P. dan Mondal, Electrocoagulation process for greywater treatment: statistical modeling, optimization, cost analysis and sludge management, Separation and Purification Technology 296 (2022) 121327, https://doi.org/10.1016/j.seppur.2022.121327.

[11] C. Wang, T. Li, G. Yu, S. Deng, Removal of low concentrations of nickel ions in electroplating wastewater using capacitive deionization technology, Chemosphere 284 (2021), https://doi.org/10.1016/j.chemosphere.2021.131341.

[12] K.E. Adou, A.R. Kouakou, A.D. Ehouman, R.D. Tyagi, P. Drogui, K. Adouby, Coupling anaerobic digestion process and electrocoagulation using iron and aluminium electrodes for slaughterhouse wastewater treatment, Scientific African 16 (2022), https://doi.org/10.1016/j.sciaf.2022.e01238.

[13] E.S.Z. El-Ashtoukhy, N.K. Amin, Y.O. Fouad, H.A. Hamad, Intensification of a new electrocoagulation system characterized by minimum energy consumption and maximum removal efficiency of heavy metals from simulated wastewater, Chemical Engineering and Processing - Process Intensification 154 (2020), https://doi.org/10.1016/j.cep.2020.108026.

[14] A.R. Vargas, C.S. Guillen, M.E. Magaña Haynes, F.Y. AlJaberi, Nickel removal from an industrial effluent by electrocoagulation in semi-continuous operation: hydrodynamic, kinetic and cost analysis, in: Results in Engineering, vol. 17, Elsevier BV, 2023 100961, https://doi.org/10.1016/j.rineng.2023.100961.

[15] A. Shahedi, A.K. Darban, A. Jamshidi-Zanjani, F. Taghipour, M. Homaee, Simultaneous removal of cyanide and heavy metals using photoelectrocoagulation, Water 15 (3) (2023) 581, https://doi.org/10.3390/w15030581. MDPI AG.

[16] E. Bazrafshan, L. Mohammadi, A. Ansari-Moghaddam, et al., Heavy metals removal from aqueous environments by electrocoagulation process– a systematic review, J Environ Health Sci Engineer 13 (2015) 74, https://doi.org/10.1186/s40201-015-0233-8.

[17] Hudori, Pengolahan air limbah laundry dengan menggunakan elektrokoagulasi, 81 p, Bandung (ID): Institut Teknologi Bandung (2008) [Tesis].

[18] F. Akbal, S. Camcı, Copper, chromium and nickel removal from metal plating wastewater by electrocoagulation, Desalination 269 (1–3) (2011) 214–222, https://doi.org/10.1016/j.desal.2010.11.001. Elsevier BV.

[19] E. Mohora, S. Rončević, J. Agbaba, A. Tubić, M. Mitić, M. Klašnja, B. Dalmacija, Removal of arsenic from groundwater rich in natural organic matter (NOM) by continuous electrocoagulation/flocculation (ECF), Separation and Purification Technology 136 (2014) 150–156, https://doi.org/10.1016/j.seppur.2014.09.006.

[20] P. Song, Z. Yang, G. Zeng, X. Yang, H. Xu, L. Wang, K. Ahmad, Electrocoagulation treatment of arsenic in wastewaters: a comprehensive review, Chem. Eng. J. (2017), https://doi.org/10.1016/j.cej.2017.02.086. Elsevier B.V.

[21] J. Kang, J. Li, C. Ma, L. Yi, T. Gu, J. Wang, S. Liu, Goethite/montmorillonite adsorption coupled with electrocoagulation for improving fluoride removal from aqueous solutions, RSC Adv. 12 (12) (2022) 7475–7484, https://doi.org/10.1039/d1ra08503d. Royal Society of Chemistry (RSC).

[22] M. Mahmood, N. Yasri, B. Fuladpanjeh-Hojaghan, E.P.L. Roberts, Influence of operating conditions on the removal of silica and hardness by continuous electrocoagulation, J. Environ. Chem. Eng. 10 (6) (2022), https://doi.org/10.1016/j.jece.2022.108899.

[23] A.S. Naje, S. Chelliapan, Z. Zakaria, S.A. Abbas, Electrocoagulation using a rotated anode: a novel reactor design for textile wastewater treatment, J. Environ. Manag. 176 (2016) 34–44, https://doi.org/10.1016/j.jenvman.2016.03.034.

[24] R.H. Petrucci, W.S. Harwood, G.F. Herring, J.D. Madura, General Chemistry : Principles and Modern Applications, ninth ed., Pearson Prentice Hall, 2007.

[25] P.V. Nidheesh, T.S.A. Singh, Arsenic removal by electrocoagulation process: recent trends and removal mechanism, Chemosphere 181 (2017) 418–432, https://doi.org/10.1016/j.chemosphere.2017.04.082. Elsevier BV.

[26] E. Jafari, M.R. Malayeri, H. Brückner, P. Krebs, Impact of operating parameters of electrocoagulation-flotation on the removal of turbidity from synthetic wastewater using aluminium electrodes, Miner. Eng. 193 (2023), https://doi.org/10.1016/j.mineng.2023.108007.

[27] R. Chang, Kimia Dasar (Edisi Ketiga), Penerbit Erlangga, 2005.

[28] R. Hermawan, M. Syafila, PENGARUH plat grafit dan TEMBAGA TERHADAP KINERJA proses pengolahan limbah cair industri batik yang MENGANDUNG logam zn menggunakan metode ELEKTROLISIS, Jurnal Tehnik Lingkungan 23 (1) (2017) 13–21, https://doi.org/10.5614/j.tl.2017.23.1.2.

[29] V. Ridantami, Recovery Timbal (Pb) Dari limbah cair hasil soil washing menggunakan proses elektrokoagulas. Tesis Program Magister, Institut Teknologi Bandung, 2021.

[30] T. Kim, T.-K. Kim, K.-D. Zoh, Removal mechanism of heavy metal (Cu, Ni, Zn, and Cr) in the presence of cyanide during electrocoagulation using Fe and Al electrodes, Journal of Water Process Engineering 33 (2020) 101109, https://doi.org/10.1016/j.jwpe.2019.101109. Elsevier BV.

[31] X. Chen, P. Ren, T. Li, J.P. Trembly, X. Liu, Zinc removal from model wastewater by electrocoagulation: processing, kinetics and mechanism, Chem. Eng. J. 349 (2018) 358–367, https://doi.org/10.1016/j.cej.2018.05.099.

[32] S.S. Moersidik, R. Nugroho, M. Handayani, Kamilawati, M.A. Pratama, Optimization and reaction kinetics on the removal of Nickel and COD from wastewater from electroplating industry using Electrocoagulation and Advanced Oxidation Processes, Heliyon 6 (2) (2020) e03319, https://doi.org/10.1016/j.heliyon.2020.e03319.

[33] A.Y. Goren, M. Kobya, Arsenic removal from groundwater using an aerated electrocoagulation reactor with 3D Al electrodes in the presence of anions, Chemosphere 263 (2021), https://doi.org/10.1016/j.chemosphere.2020.128253.

[34] Y. Hu, L. Zhou, J. Zhu, J. Gao, Efficient removal of polyamide particles from wastewater by electrocoagulation, Journal of Water Process Engineering 51 (2023), https://doi.org/10.1016/j.jwpe.2022.103417.

[35] J. Lu, R. Fan, H. Wu, W. Zhang, J. Li, X. Zhang, D. Liu, Simultaneous removal of Cr(VI) and Cu(II) from acid wastewater by electrocoagulation using sacrificial metal anodes, J. Mol. Liq. 359 (2022), https://doi.org/10.1016/j.molliq.2022.119276.

[36] A. Akyol, Treatment of paint manufacturing wastewater by electrocoagulation, Desalination 285 (2012) 91–99, https://doi.org/10.1016/j.desal.2011.09.039. Elsevier BV.

[37] S. Garcia-Segura, M.M.S.G. Eiband, J.V. de Melo, C.A. Martínez-Huitle, Electrocoagulation and advanced electrocoagulation processes: a general review about the fundamentals, emerging applications and its association with other technologies, J. Electroanal. Chem. 801 (2017) 267–299, https://doi.org/10.1016/j.jelechem.2017.07.047. Elsevier BV.

[38] K. Xiao, D. Huang, C. Kang, S. Sun, Removal of tetracyclines from aqueous solutions by electrocoagulation/pecan nutshell coupling processes: synergistic effect and mechanism, Water Sci. Technol. 82 (4) (2020) 683–694, https://doi.org/10.2166/wst.2020.367.

[39] S. Kumari, R.N. Kumar, How effective aerated continuous electrocoagulation can be for tetracycline removal from river water using aluminium electrodes? Chemosphere 305 (2022) 135476 https://doi.org/10.1016/j.chemosphere.2022.135476. Elsevier BV.

[40] Y. Liu, G. Liu, H. Wang, P. Wu, Q. Yan, D.V. Vayenas, Elongation the duration of steel anode with polypyrrole modification during the electrocoagulation treatment process of electroplating wastewater, J. Environ. Chem. Eng. 9 (2) (2021), https://doi.org/10.1016/j.jece.2020.104969.

[41] L. Singh Thakur, R. Baghel, A. Sharma, S. Sharma, S. verma, H. Parmar, P. Mondal, Simultaneous removal of lead, chromium and cadmium from synthetic water by electrocoagulation: optimization through response surface methodology, Mater. Today: Proc. 72 (2023) 2697–2704, https://doi.org/10.1016/j.matpr.2022.09.031. Elsevier Ltd.

[42] A. Doggaz, A. Attour, M. Le Page Mostefa, M. Tlili, F. Lapicque, Iron removal from waters by electrocoagulation: investigations of the various physicochemical phenomena involved, Separation and Purification Technology 203 (2018) 217–225, https://doi.org/10.1016/j.seppur.2018.04.045.

[43] F.E. Titchou, H. Zazou, H. Afanga, J. El Gaayda, R.A. Akbour, M. Hamdani, Removal of Persistent Organic Pollutants (POPs) from water and wastewater by adsorption and electrocoagulation process, in: Groundwater for Sustainable Development, vol. 13, Elsevier BV, 2021 100575, https://doi.org/10.1016/j.gsd.2021.100575.